Interdomain Conformational Changes in Akt Activation Revealed by Chemical Cross-linking and Tandem Mass Spectrometry*

Bill X. Huang and Hee-Yong Kim‡

Akt, a serine/threonine kinase, plays a critical role in cell survival. Upon growth factor receptor stimulation, cytosolic Akt is recruited to the plasma membrane by phospholipid binding and activated through phosphorylation at Thr^{308} and Ser^{473}. Although crystal structures for the parts of Akt have been reported, neither the three-dimensional structure of the whole molecule nor sequential conformational changes during activation have been demonstrated. In this study, we demonstrated that Akt undergoes dramatic interdomain conformational changes during activation processes by probing the three-dimensional structure of full-length Akt in solution using chemical cross-linking and tandem mass spectrometry. The cross-linking results not only provided new structural information but also revealed distinctive spatial arrangements of individual domains in the Akt molecule in resting, membrane-interacted, phosphorylated, and substrate-bound states. Our data allowed a new model for stepwise interdomain conformational changes in Akt activation sequence, setting a stage for the further investigation on Akt-membrane, Akt-protein, and/or Akt-drug interactions in solution to understand molecular mechanisms involved in physiological and pathophysiological processes of cell survival. ***Molecular & Cellular Proteomics 5:1045–1053, 2006.***

The serine/threonine kinase Akt (protein kinase B (PKB)[1]) is a central mediator for many cellular responses involved in cell survival, differentiation, proliferation, and insulin signaling (1, 2). In human there are two major Akt isomers, Akt1 (PKB$_\alpha$) and Akt2 (PKB$_\beta$) (3), which exhibit approximately 80% amino acid sequence identity. Each isomer possesses an N-terminal pleckstrin homology (PH) domain (residues 1–113), a kinase domain (residues 150–408) that is similar to those found in other AGC members such as cAMP-dependent protein kinase and protein kinase C, and a C-terminal regulatory domain (residues 409–480) containing a hydrophobic motif (Fig. 1) (4–6). During the activation process, cytosolic Akt is recruited to the plasma membrane through the interaction of its PH domain with phosphatidylinositol 3,4,5-trisphosphate (PIP$_3$), which is generated by phosphatidylinositol 3-kinase in response to the growth factor receptor stimulation. It is thought that the membrane interaction results in conformational changes of Akt, exposing a pair of residues, Thr^{308} at the activation loop of the kinase domain and Ser^{473} at the hydrophobic motif of the regulatory domain, for phosphorylation by the phosphoinositide-dependent kinase 1 (PDK1) and a putative kinase PDK2, respectively (7–10). It has been demonstrated that the phosphorylation at both Thr^{308} and Ser^{473} is required for the full activation of Akt (11). The phosphorylated active Akt in turn phosphorylates downstream effectors such as GSK3, PFK2, and BAD (12, 13).

Structural studies to understand the molecular mechanism for the activation and regulation of Akt have been carried out mostly using x-ray crystallography. To date, high resolution crystal structures of Akt have been reported for the Akt1 PH domain with and without PIP$_3$ binding (6, 14), the unliganded inactive Akt2 kinase domain (15), and the kinase domain of active Akt2 complexed with GSK3β peptide and an ATP analog (16). Studies using NMR or circular dichroism have also provided supportive information on the conformation of Akt bound to PIP$_3$ (14, 17). In addition, fluorescence lifetime imaging microscopy has been used to monitor *in situ* conformational changes in response to growth factor stimulation (18). Nevertheless up to now these methods demonstrated neither the 3D structure of the whole Akt molecule nor sequential conformational changes involved in the activation process. Apparently an alternative technique to explore the 3D structures of the full-length Akt is required for further understanding of this enzyme. Chemical cross-linking combined with MS has recently emerged as a sensitive tool for probing 3D structure of proteins in solution (19–23). Determination of the cross-linked amino acid residues by MS provides spatial distance information that has been proven valuable for the elucidation of protein structural changes due to protein-ligand and protein-protein interactions in more physiologically rele-

From the Section of Mass Spectrometry, Laboratory of Membrane Biophysics and Biochemistry, NIAAA, National Institutes of Health, Bethesda, Maryland, 20892-9410

Received, January 18, 2006, and in revised form, March 8, 2006
Published, MCP Papers in Press, March 9, 2006, DOI 10.1074/mcp.M600026-MCP200

[1] The abbreviations used are: PKB, protein kinase B; PIP$_3$, phosphatidylinositol 3,4,5-trisphosphate; PH, pleckstrin homology; 3D, three-dimensional; BS^3, bis(sulfosuccinimidyl) suberate; DSS, disuccinimidyl suberate; DSG, disuccinimidyl glutarate, AMP-PNP, adenylyl imidodiphosphate; PS, 1-palmitoyl-2-oleoyl-*sn*-glycero-3-phosphoserine; PC, 1-stearoyl-2-linoleoyl-*sn*-glycero-3-phosphocholine; PE, 1-stearoyl-2-oleoyl-*sn*-glycero-3-phosphoethanolamine; GSK3, glycogen synthase kinase 3; PDK, phosphoinositide-dependent kinase.

vant conditions (24–29). This approach complements, and sometimes is a viable alternative to, x-ray crystallography, particularly when a whole protein molecule cannot be readily crystallized.

In the present study, we probed the 3D structures of full-length Akt1 (Akt hereafter) in solution using lysine-specific bifunctional cross-linkers with varying spacer arm lengths and chemistry, including bis(sulfosuccinimidyl) suberate (BS^3), disuccinimidyl suberate (DSS), and disuccinimidyl glutarate (DSG), to provide spatial distance constraints between Akt domains yet to be established. To gain insights into the Akt activation mechanism, Akt conformation at different activation stages, including inactive, membrane-interacted, phosphorylated, and substrate-bound states was probed. The cross-linked lysine residues were unambiguously determined by tandem mass spectrometry with static nano-ESI and HPLC/nano-ESI. ^{18}O labeling of tryptic digests (30) was used to further confirm the through-space cross-linked peptides (22, 29, 31) and to compare the peak intensity of the cross-linked peptides produced from Akt at various stages of activation. We identified two interdomain cross-linked pairs that allowed us to monitor interdomain conformational changes during activation. These cross-linked pairs also provided spatial distance constraints between domains that are not available from the crystal structure. Our results demonstrate for the first time that Akt undergoes distinctive interdomain conformational changes at each step of activation and substrate binding.

EXPERIMENTAL PROCEDURES

Chemicals—Inactive and phosphorylated active Akt1 with 90% purity was purchased from Upstate Cell Signaling Solutions (Lake Placid, NY) or Calbiochem. BS^3, DSS, and DSG were purchased from Pierce. Modified trypsin was purchased from Promega (Madison, WI). K-LISA Akt activity kit and adenylyl imidodiphosphate (AMP-PNP) tetralithium salt were purchased from Calbiochem. Phospho-Thr^{308} and -Ser^{473} Akt antibodies were purchased from Cell Signaling Technology (Beverly, MA). GSK3β peptide substrate (GRPRTTSFAE) was purchased from AnaSpec Inc. (San Jose, CA). 1-Palmitoyl-2-oleoyl-*sn*-glycero-3-phosphoserine (PS), 1-stearoyl-2-linoleoyl-*sn*-glycero-3-phosphocholine (PC), and 1-stearoyl-2-oleoyl-*sn*-glycero-3-phosphoethanolamine (PE) were purchased from Avanti Polar Lipids (Alabaster, AL). L-α-D-*myo*-Phosphatidylinositol 3,4,5-trisphosphate was purchased from A. G. Scientific, Inc. (San Diego, CA). HEPES buffer solution was purchased from Invitrogen. Pure water was obtained from a Gemini high purity water system (West Berlin, NJ). $H_2{}^{18}O$ (99%) was purchased from Isotec (Miamisburg, OH). Dimethyl sulfoxide (Me_2SO) was purchased from Sigma. Other chemicals were purchased from Mallinckrodt.

Cross-linking Reaction and Tryptic Digestion—Akt samples at 5 μM were dialyzed overnight against 50 mM HEPES (pH 7.8) containing 50 mM NaCl at 4 °C to remove the primary amine-containing Tris-HCl buffer. Aliquots before or after dialysis were used to measure the Akt activity and subjected to Western blotting against phosphospecific Akt antibodies. The Akt activity measured before and after dialysis was identical, although the protein lost ~30% of its activity under the conditions used in this study. The samples were incubated with a 50 molar excess of freshly prepared BS^3 (in pH 5.0 sodium citrate), DSS, or DSG (in Me_2SO at a final concentration of 1% in the reaction mixture) at room temperature for 5 min. At this cross-linking condition intermolecular cross-linked dimers or multimers were not observed according to the SDS-PAGE separation data. The cross-linking reaction was quenched with 1 M Tris-HCl (pH 7.4). The samples were digested with trypsin at 37 °C for 20 h using a trypsin to protein ratio of 1:20. Alternatively samples were reduced with dithiothreitol and alkylated with iodoacetamide before tryptic digestion. For ^{18}O labeling of tryptic digests, samples were dialyzed against water, dried using a vacuum centrifuge, and reconstituted in pure water or 99% $H_2{}^{18}O$ with 5% acetonitrile prior to the digestion with trypsin (29, 31).

Akt Kinase Assay and Western Blot—The kinase activity was measured with a K-LISA Akt activity kit that uses streptavidin-coated 96-well plates and a biotinylated peptide substrate (GRPRTSSFAEG) according to the manufacturer's instructions (Calbiochem). The phosphorylation states of Akt were examined by Western blots using phospho-Thr^{308} and -Ser^{473} Akt antibodies.

Preparation of Unilamellar Vesicles and Akt-Liposome Interaction—Unilamellar vesicles containing PE, PC, PS, and PIP_3 at a ratio of 50:18:30:2 were prepared according to the method reported previously (32). After dialysis overnight against 50 mM HEPES (pH 7.8) containing 50 mM NaCl at 4 °C, inactive Akt was incubated with the freshly prepared unilamellar vesicles at 37 °C for 1 h (33).

Complex Formation with GSK3β Peptide and AMP-PNP—Active or inactive Akt at 5 μM was incubated with equivalent volumes of 50 μM GSK3β peptide substrate and 200 μM AMA-PNP (16) at room temperature for 1 h and dialyzed overnight against 50 mM HEPES (pH 7.8) containing 50 mM NaCl at 4 °C. After treatment with cross-linkers, aliquots were subjected to tryptic digestion followed by mass spectrometric analysis in accordance with the procedures described under "Cross-linking Reaction and Tryptic Digestion."

Off-line Static Nano-ESI Mass Spectrometric Analysis—Tryptic digests were desalted with a C_{18} ZipTip (Millipore Corp.) prior to analysis by a high resolution QSTAR pulsar Qq-TOF mass spectrometer (Applied Biosystems/MDS Sciex, Toronto, CA) equipped with a nano-electrospray ionization source. The ion source voltage was set at 1100 V in the positive ion mode. A full mass spectrum was acquired over an *m/z* range of 500–2000, and the ions of interest were subjected to CID using high purity argon to obtain tandem MS data. The performance of the instrument featured resolution greater than 8000 and mass accuracy with less than 30 ppm error in both full MS and tandem MS mode. The *m/z* data were reconstructed to generate mass spectra using Analyst QS software (Applied Biosystems/MDS Sciex).

HPLC/Nano-ESI Mass Spectrometric Analysis—HPLC/nano-ESI MS analysis was performed on an Agilent ion trap mass spectrometer (XCT) equipped with an Agilent 1100 nanoflow HPLC system. Peptides were trapped in a C_{18} enrichment column (Zorbax 300SB C_{18}, 0.3 $\times$ 5 mm, Agilent, Wilmington, DE) and then separated on a Zorbax 300SB C_{18} column (75 μm $\times$ 150 mm, 3.5 μm) using a mobile phase that contained solvent A (0.1% formic acid in water) and solvent B (0.1% formic acid in acetonitrile) at a flow rate of 300 nl/min. The mobile phase composition was held initially at 3% B for 5 min and gradually changed to 15, 45, and 85% B at 8, 50, 55 min, respectively, and held at 85% for 5 min. The data-dependent automatic scan mode ("Auto-MS^2") was used. The capillary voltage was set to 1750 V. The mass spectrometer was scanned from 300 to 2000 *m/z* range.

Analysis of the Cross-linked Peptides—Protein Analysis Work Sheet (PAWS) was used to assign the mass values of tryptic peptides. The emerging cross-linked peptides were identified by comparing the mass spectra of tryptic peptides obtained from modified sample with those from the unmodified control. Tandem MS data for the cross-linked peptides were manually interpreted with the assistance of Protein Analysis Work Sheet and Analyst QS software (Applied Biosystem/MDS Sciex).

RESULTS AND DISCUSSION

Determination of the Cross-linked Residues in Inactive Akt—The tryptic peptides of Akt detected by nano-ESI MS represented more than 85% of sequence coverage (Fig. 1). The cross-linked peptide peaks were distinguished by comparing the static nano-ESI mass spectra obtained from cross-linker-modified Akt with the mass spectrum from the non-modified control. Fig. 2 shows reconstructed mass spectra of the tryptic digests from the control and modified Akt. Twelve newly emerging peaks were identified in Akt samples modified with DSS. Modification with BS^3, a hydrophilic analog of DSS, yielded the same results, indicating that all the modified lysine residues are exposed on the surface and easily accessible by both hydrophilic and hydrophobic cross-linking reagents. DSG, which contains a cross-linking arm ($C_5H_6O_2$) shorter by $(CH_2)_3$ than that of DSS ($C_8H_{12}O_2$), was used to refine distance constraints for the observed lysine pairs. In the DSG-modified sample, all but one of the newly emerging peaks were observed at mass values 42 Da lower than those observed in the DSS-modified sample. The through-space cross-linked peptide peaks, which are more valuable with respect to protein folding, were further confirmed by ^{18}O labeling of the tryptic digests. When hydrolyzed in $H_2{}^{18}O$, each C terminus of a tryptic peptide incorporates two ^{18}O atoms (30). Thus, internally cross-linked or end-capped peptides show a 4-Da mass shift, whereas the through-space cross-linking between two peptides results in an 8-Da mass increase (22, 29, 31). The peptides with masses of 2458, 3465, and 3623 Da, reconstructed from the corresponding multiply charged ions, increased 8 Da in mass when labeled with ^{18}O, indicating that these peptides resulted from through-space cross-linking. The rest of the emerging peptides showed 4-Da mass shifts indicating that they originated from the end capping or internal cross-linking.

Among the three through-space cross-linked pairs observed in DSS- and BS^3-modified Akt, the peaks with 2458 and 3465 Da turned out to be interdomain cross-linked peptide pairs according to the MS/MS analysis (Fig. 3). Fig. 3 (*top*) shows the MS/MS spectrum from the peptide with mass of 2458 Da (reconstructed from the triply charged ion at *m/z* 820.4) observed in the DSS- and BS^3-modified samples. The spectrum revealed that this peptide resulted from the cross-linking between the segments Tyr^{26}–Lys^{39} and Asp^{387}–Arg^{391}

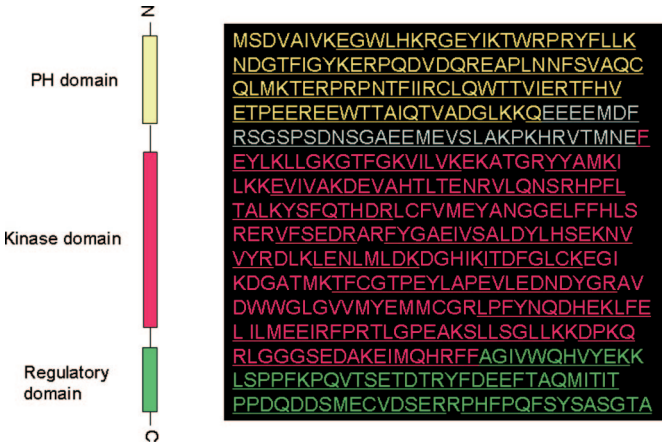

FIG. 1. **Primary sequence of Akt1 showing three domains, the N-terminal PH domain (residues 1–113, marked in *yellow*), the kinase domain (residues 150–408, marked in *red*), and the C-terminal regulatory domain (residues 409–480, marked in *green*).** Mass spectrometric detection of the tryptic digests covered 85% of the amino acid sequence (*underlined*) under our experimental conditions.

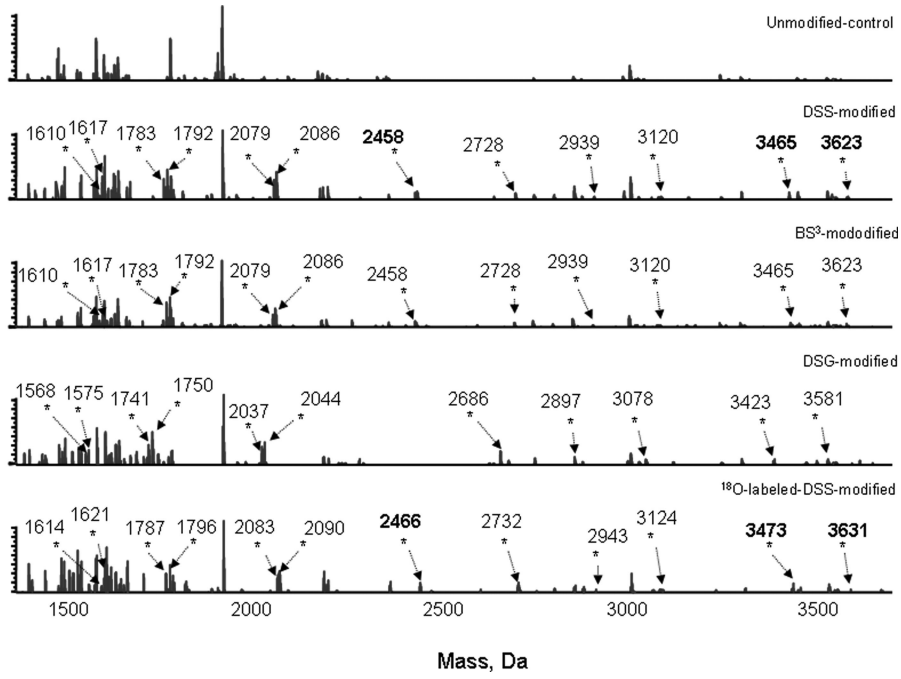

FIG. 2. **Nano-ESI-Qq-TOF reconstructed mass spectra of tryptic digests from unmodified or cross-linker-modified inactive Akt samples.** Newly emerging cross-linked peptides (marked with *asterisks*) were identified in modified samples. ^{18}O labeling facilitated the identification of three through-space cross-linked peptides by showing an 8-Da mass shift as demonstrated by DSS-modified samples (mass shifted pairs are shown in *bold*).

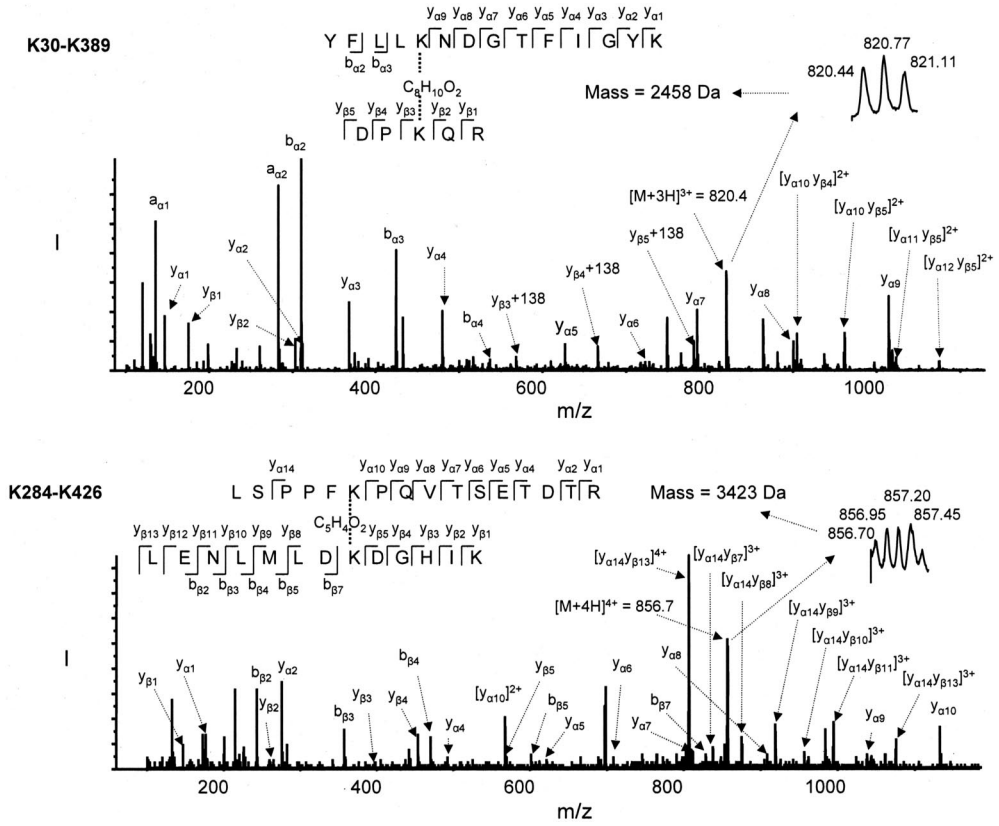

FIG. 3. **MS/MS analysis of the cross-linked peptides with mass of 2458 Da (*top*) and 3423 Da (*bottom*) depicted in Fig. 2.** The mass values of the peptides were derived from the corresponding multiply charged ions (*insets*). The sequences of the peptides were assigned with *single letter* abbreviation based on the fragment ions observed for the cross-linked peptide segments. N-terminal b ions and C-terminal y ions resulting from the amide bond cleavage as well as N-terminal a ions due to the cleavage of C–C bond are labeled. *Top*, the MS/MS spectrum indicated that two peptide segments, Tyr^{26}–Lys^{39} (labeled with α) and Asp^{387}–Arg^{391} (labeled with β), were cross-linked at Lys^{30} and Lys^{389} via $C_8H_{10}O_2$. *Bottom*, the MS/MS spectrum indicated that Lys^{284} of the peptide segment Leu^{277}–Lys^{289} (labeled with β) linked to Lys^{426} of Leu^{421}–Arg^{436} (labeled with α) via $C_5H_4O_2$, the cross-linking bridge from DSG.

with Lys^{30} of the PH domain linked to Lys^{389} of the kinase domain via $C_8H_{10}O_2$ (derived from $C_8H_{12}O_2$, the cross-linking arm of DSS, with two hydrogen atoms subtracted due to cross-linking). The Lys^{30}-Lys^{389} cross-linking observed in the DSS-modified sample (2458 Da) was not detected from the DSG-modified Akt (supposedly 2416 Da). The sequence assignment was based on the fragment ions observed for both segments and the ions containing $C_8H_{10}O_2$. The N-terminal "b" or "a" ions and C-terminal "y" ions from each segment were separately labeled using subscripts α and β (34). The MS/MS analysis also revealed the other interdomain cross-linking between Lys^{284} of the kinase domain and Lys^{426} of the regulatory domain that was detected at 3465 and 3423 Da after modification with DSS (or BS^3) and DSG, respectively (Fig. 2). The MS/MS spectrum indicated that the peak at 3423 Da (reconstructed from the quadruply charged ion at *m/z* 856.7) consisted of the peptide segments Leu^{277}–Lys^{289} and Leu^{421}–Arg^{436} cross-linked between Lys^{284} and Lys^{426} via $C_5H_4O_2$ (Fig. 3, *bottom*). Consistently the MS/MS spectra of the corresponding cross-linked peptide detected with mass of 3465 Da in the DSS- or BS^3-modified samples revealed the same cross-linking with a longer bridge of $C_8H_{10}O_2$ (data not shown).

Probing 3D Structure of Inactive Akt Using Cross-linking Data—Table I summarizes all the cross-linked peptides identified and characterized by tandem MS, including two interdomain and five intradomain cross-linked pairs as well as five end-capped peptides. The presence of all these modified peptide peaks identified by static nano-ESI MS was also unambiguously confirmed by HPLC/MS/MS (data not shown). The α-carbon distance constraints for each cross-linked lysine pair determined in the present study are shown in Table I. Table I also lists the α-carbon distances between the corresponding lysine residues from the crystal structures of the inactive Akt1 PH domain (Protein Data Bank entry 1unp) or the kinase domain of inactive Akt2 (Protein Data Bank entry 1mrv) as the reference.

Our results indicated that all the cross-linked or end-capped lysine residues were exposed on the surface because they were modified by both hydrophobic DSS and its hydrophilic analog BS^3. The residues Lys^{189} and Lys^{268}, which were missing in the crystal structure due to inadequate resolution of

TABLE I
Cross-linked lysine residues in inactive Akt molecule
PH, the PH domain; kin, the kinase domain; reg, the regulatory domain; ND, not detected; NA, not applicable; mod., modified.

Cross-linked lysine pairs or end-capped lysine residues identified by MS/MS	Mass of the cross-linked tryptic peptides	Type of cross-linking	BS^3 -mod.	DSS-mod.	DSG-mod.	Distance constraint of cross-linked α-carbons	α-Carbon distance in the crystal structure
	Da					*Å*	*Å*
Lys^{111}(PH)-Lys^{112}(PH)	3120[a] (3078)[b]	Intradomain	+	+	+	≤20	3.8[c]
Lys^{214}(kin)-Lys^{284}(kin)	3623 (3581)	Intradomain	+	+	+	≤20	17.9[d]
Lys^{158}(kin)-Lys^{163}(kin)	1610 (1568)	Intradomain	+	+	+	≤20	4.0[d]
Lys^{30}(PH)-Lys^{39}(PH)	2939 (2897)	Intradomain	+	+	+	≤20	17.9[c]
Lys^{284}(kin)-Lys^{426}(reg)	3465 (3423)	Interdomain	+	+	+	≤20	7.8[d]
Lys^{30}(PH)-Lys^{389}(kin)	2458 (ND)	Interdomain	+	+	−	20–24	NA
Lys^{377}(kin)-Lys^{385}(kin)	1792 (1750)	Intradomain	+	+	+	≤20	12.1[d]
Lys^{20}(PH)	1617 (1575)	Capping	+	+	+		
Lys^{189}(kin)	2079 (2037)	Capping	+	+	+		
Lys^{268}(kin)	2728 (2686)	Capping	+	+	+		
Lys^{400}(kin)	1783 (1741)	Capping	+	+	+		
Lys^{420}(reg)	2086 (2044)	Capping	+	+	+		

[a] Using DSS or BS^3.
[b] Using DSG.
[c] Obtained from the Protein Data Bank entry 1unp.
[d] Obtained from the equivalent lysine residues in inactive Akt2 (Protein Data Bank entry 1mrv).

the electron density (15) or absence of the equivalent lysine residue, respectively, were also end-capped, revealing that these residues are in the easily accessible environment. The spatial distance constraint generated by DSS (or BS^3) or DSG for cross-linked lysine pairs is 24 and 20 Å, respectively, considering the mobility of the side chains of lysine residues (19, 22). The cross-linking was observed for Lys^{30}-Lys^{39}, Lys^{111}-Lys^{112}, Lys^{158}-Lys^{163}, Lys^{214}-Lys^{284}, Lys^{284}-Lys^{426}, and Lys^{377}-Lys^{385} not only with DSS and BS^3 but also with DSG, a shorter cross-linker, indicating that the distance between the α-carbons of the lysine residues in each pair is less than 20 Å. This result was in agreement with the x-ray crystallographic data reported for the PH domain of Akt1 and the kinase domain of Akt2. An exception was observed for the interdomain cross-linking between Lys^{30} of the PH domain and Lys^{389} of the kinase domain that was detected only with the longer cross-linkers DSS and BS^3 but not in the DSG-modified sample, suggesting that the distance between the α-carbons of this lysine pair is greater than 20 Å but less than 24 Å. This interdomain distance constraint, which is not yet available from the existing x-ray crystallographic data, should be valuable for modeling a full-length Akt molecule. The presence of the two interdomain cross-linked pairs Lys^{30}-Lys^{389} and Lys^{284}-Lys^{426} indicated a spatial proximity between the PH and the kinase domains as well as the regulatory and kinase domains in the Akt structure, suggesting that inactive Akt exists as a folded molecule with the PH and regulatory domains covering parts of the kinase domain.

Conformational Changes of Akt upon Membrane Interaction, Phosphorylation, and Substrate Binding—The two interdomain cross-linked pairs Lys^{30}-Lys^{389} and Lys^{284}-Lys^{426} allowed us to monitor Akt conformation at different stages of activation, including inactive, membrane-interacted, phosphorylated, and substrate-bound states. The activity and phosphorylation states of active Akt were evaluated by K-LISA activity assay, Western blotting, and mass spectrometry (Fig. 4). Only the active Akt showed kinase activity and phosphorylation at both Thr^{308} and Ser^{473} determined by the K-LISA assay and Western blotting described under "Experimental Procedures." Consistently the tryptic peptides containing phosphorylated Thr^{308} (3362 Da) and Ser^{473} (1732 Da) were detected only in the mass spectrum of the active Akt sample. In comparison with the inactive Akt, non-phosphorylated tryptic peptides containing either Thr^{308} or Ser^{473} decreased by ~80% in the active sample according to the quantitation based on ^{18}O labeling and/or the intensity comparison using a known unmodified tryptic peptide (data not shown).

To observe the conformational changes upon membrane interaction, inactive Akt was incubated with liposomes containing PE/PC/PS/PIP_3 at a ratio of 50:18:30:2, which approximated a lipid composition in the inner leaflet of the neuronal plasma membrane under a stimulated condition, considering the fact that PS is exclusively localized in the inner plasma membrane, whereas PC is mostly on the outside. Under this condition, the two interdomain cross-linked pairs Lys^{30}-Lys^{389} and Lys^{284}-Lys^{426} were no longer observed within 24-Å spatial distance constraint (Fig. 5, *top*). Because individual modification of these lysine residues was observed under this condition (data not shown), it is clear that these residues were still accessible, suggesting that the cross-linking partners in Lys^{30}-Lys^{389} and Lys^{284}-Lys^{426} moved further away from each other upon membrane interaction. In the phosphorylated active form of Akt,

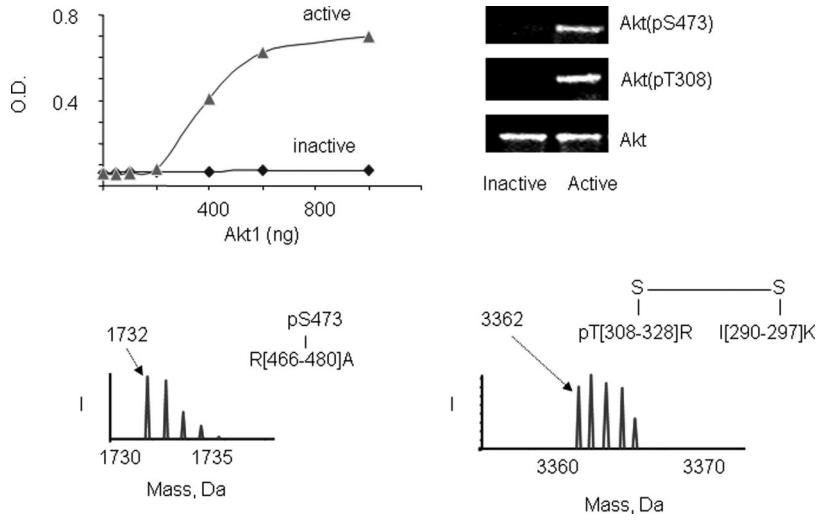

FIG. 4. **Evaluation of the kinase activity by K-LISA activity assay and the phosphorylation states by Western blotting (*top*) and mass spectrometry (*bottom*).** Tryptic peptides containing phosphorylated Thr[308] (3362 Da) and Ser[473] (1732 Da) were detected only in the mass spectrum of the active Akt samples. *pS*, phosphoserine; *pT*, phosphothreonine.

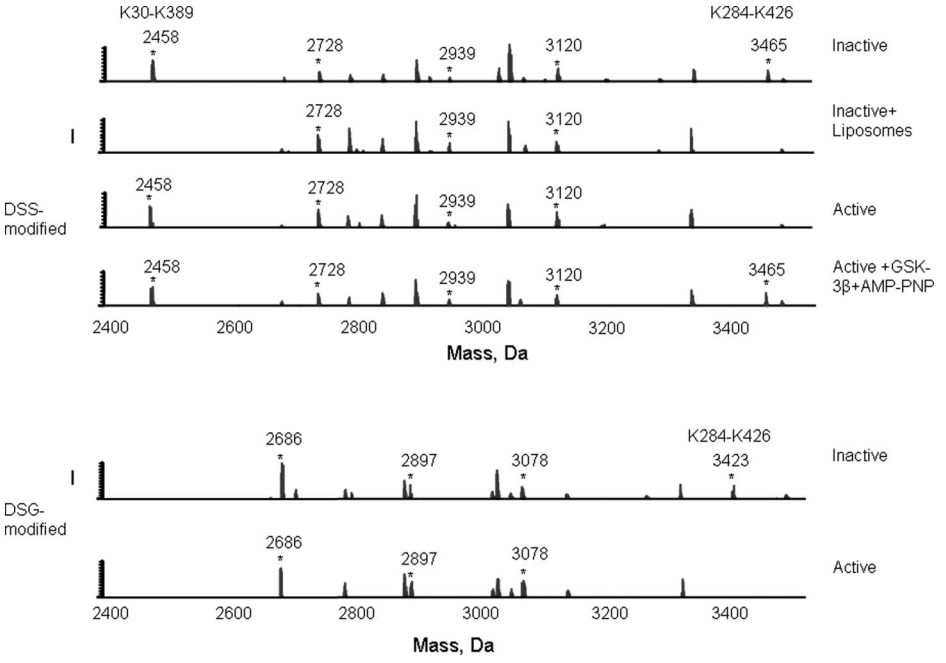

FIG. 5. **Nano-ESI-Qq-TOF reconstructed mass spectra from modified Akt samples at different activation stages.** *Top*, in DSS-modified samples, the peaks with masses of 2458 and 3465 Da representing the interdomain cross-linked pairs Lys[30]-Lys[389] and Lys[284]-Lys[426], respectively, were detected depending on the activation state. *Bottom*, in DSG-modified samples, the peak representing the cross-linked pair Lys[284]-Lys[426] was observed in inactive Akt but not in active Akt, whereas Lys[30]-Lys[389] (supposedly with mass of 2416 Da) was not observed in both cases. Cross-linked peptides are marked with *asterisks*.

Lys[284]-Lys[426] cross-linking was still missing, but Lys[30]-Lys[389] cross-linking reappeared, indicating that the proximity between Lys[30] and Lys[389] was regained due to phosphorylation. When cross-linked with DSG, Lys[30]-Lys[389] (supposedly with mass of 2416 Da) was not observed in the active form (Fig. 5, *bottom*), indicating that the spatial distance between Lys[30] and Lys[389] remained 20–24 Å as was the case with the inactive Akt.

An analytical concern regarding the conclusion drawn from the comparison of peak abundance between non-identical complex mixtures is that peaks of interest may be reduced or eliminated due to ion suppression in different samples. To undoubtedly confirm the observed changes of the peaks, we took advantage of the ^{18}O labeling technique. The cross-linker-modified inactive Akt sample digested in $H_2{}^{18}O$ was mixed with the modified Akt samples from different activation stages digested in normal $H_2{}^{16}O$ water, and the mixture was subjected to MS analysis. As an example, the mass spectrum is shown in Fig. 6 for the DSS-modified ^{18}O-labeled digest of the inactive Akt mixed with the ^{16}O digest of the DSS-modified active Akt at a ratio of 1:1. As expected the peak intensity ratio of the non-cross-linked tryptic peptide with mass of 2886 Da (Thr[87]–Lys[111]) in $H_2{}^{16}O$ digest to its counterpart of 2890 Da in $H_2{}^{18}O$ digest was ~1:1. A similar ratio was observed for the cross-linked pair of Lys[30]-Lys[389] (2458 *versus* 2466 Da) or the peak end-capped at Lys[268] (2728 *versus* 2732 Da), indicating the presence of these cross-linked pairs in both inactive and active forms at a comparable level. However, Lys[284]-Lys[426] cross-linking was detected only with the inactive Akt at

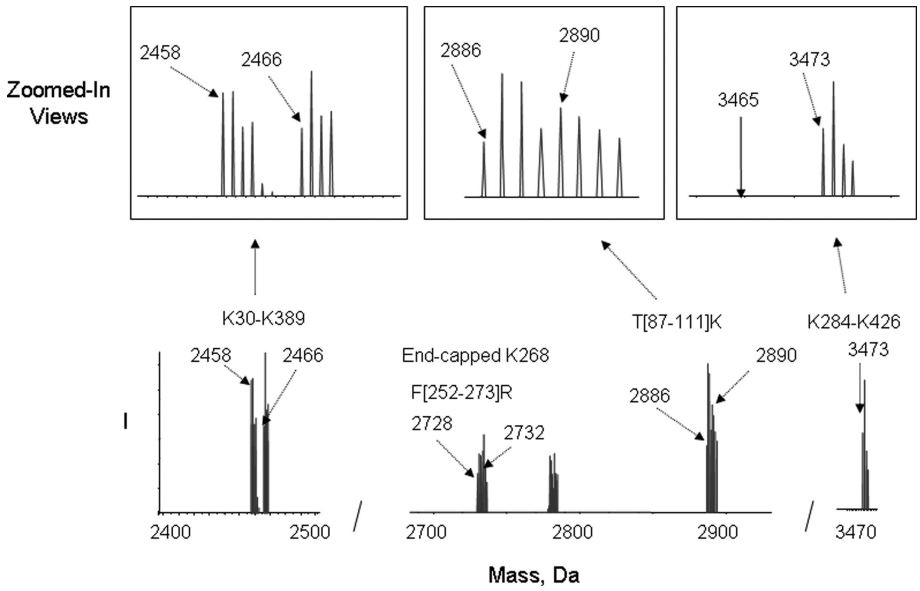

FIG. 6. **Representative nano-ESI-Qq-TOF reconstructed mass spectrum obtained from the DSS-modified ^{18}O-labeled tryptic digests of the inactive Akt mixed with the ^{16}O digests of the active Akt at a ratio of 1:1.** The zoomed-in views of the spectra are also shown. The peak with mass of 3465 Da representing the cross-linking of Lys^{284}-Lys^{426} from active Akt (^{16}O digests) was not detected in the spectrum. Other peaks including non-cross-linked peptide Thr^{87}–Lys^{111} (*T[87–111]K*), end-capped peptide Phe^{252}–Arg^{273} (*F[252–273]R*) with Lys^{268} capping, and Lys^{30}-Lys^{389} were detected with intensities comparable to those from inactive Akt (^{18}O digests).

3473 Da (^{18}O digest) and was not detected at 3465 Da with the active sample digested in $H_2{}^{16}O$ with the instrumental sensitivity of our current setting. These results were further confirmed by LC/MS/MS (data not shown).

Conformational changes of Akt also occurred when active Akt was bound to substrates. The substrate binding status was indicated in the mass spectra obtained from the tryptic digest of the active Akt after the incubation with substrates. Binding the GSK3β peptide substrate and AMP-PNP, an ATP analog, to Akt interfered with the tryptic digestion at Lys^{307}, resulting in the miscleavage at Lys^{307}. A new peak with mass of 3965 Da was identified by MS/MS as Asp^{302}–Arg^{328} and Lys^{290}–Ile^{297} linked via a disulfide bond between Cys^{310} and Cys^{296} with phosphorylation at Thr^{308} (data not shown). This peak was not observed in the tryptic digest either from active Akt alone (phosphorylation at Thr^{308} alone did not interfere the tryptic hydrolysis at Lys^{307}) or from inactive Akt mixed with GSK3β peptide and AMP-PNP (as the corresponding unphosphorylated peak at 3885 Da), indicating that the substrate was indeed bound to the kinase loop (residues 296–311) region specifically in active Akt. In the substrate-bound form, Lys^{284}-Lys^{426} cross-linking (3465 Da), which was not observed in the unliganded active Akt form, emerged again with DSS (Fig. 5, *top*) as well as BS^3 and DSG (data not shown).

The intra-PH domain and intra-kinase domain cross-linking, including Lys^{30}(β2)-Lys^{39}(β3/β4 loop), Lys^{111}(α-helix)-Lys^{112}-(α-helix), Lys^{158}(β1)-Lys^{163}(β2), Lys^{214}(β4)-Lys^{284}(β7/β8 loop), and Lys^{377}(αH)-Lys^{385}(αH/αI loop), remained unaltered after membrane interaction, phosphorylation, or substrate binding. Although the local conformational changes within each domain could not be probed by this approach due to the low resolution in probing distance constraints using current cross-linkers, the changes in the interdomain cross-linking observed in this study clearly indicated that arrangements of individual domains were profoundly affected during activation processes.

Proposed Scheme for Interdomain Conformational Changes in Akt Activation—From the currently available biochemical data (1, 5) it has been proposed that PIP_3 interacts with the PH domain of Akt, exposing Thr^{308} and Ser^{473}, which in turn are subjected to phosphorylation by upstream kinases for activation (1, 7). For example, mutating the PH domain abolishes the phosphorylation and activation of Akt by the upstream kinases even in the presence of PIP_3 (7). On the other hand, truncation of the PH domain results in phosphorylation and activation of Akt without PIP_3 (7). These data suggest that the PH domain may block the access of the upstream kinase to the phosphorylation sites of Akt, and the binding of PIP_3 to the PH domain is a way to remove such structural hindrance. Additionally an *in situ* study using fluorescence lifetime imaging microscopy has suggested that Akt undergoes a conformational change at the plasma membrane upon growth factor stimulation in intact cells (18). Nevertheless no structural evidence is available concerning the alteration of interdomain arrangements accompanying the activation sequence. The lack of the cross-linking of Lys^{30}-Lys^{389} and Lys^{284}-Lys^{426} in the liposome-interacted Akt molecule observed in our study provided evidence that Akt indeed exists with an open conformation upon phospholipid binding, presumably exposing the phosphorylation sites. Our data also revealed that this membrane-induced open conformation was subsequently altered by phosphorylation. The presence of Lys^{30}-Lys^{389} in both inactive and phosphorylated forms suggests that the spatial arrangements of the PH and kinase domains are similar in both active and inactive forms. The fact that this cross-linking first disappeared due to membrane interaction before it was detected again in the phosphorylated form strongly suggests that phosphorylation triggered the separation of the PH domain from the membrane. The absence of the

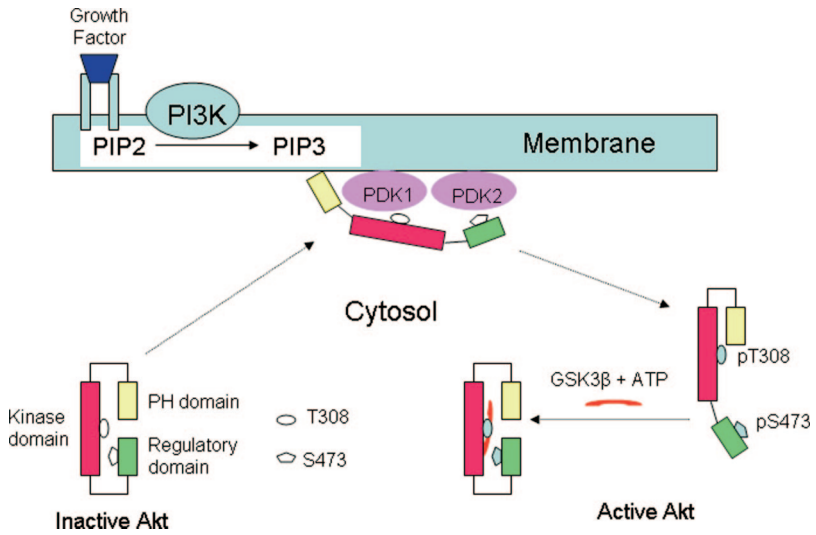

FIG. 7. **Schematic model for interdomain conformational changes accompanying Akt activation and substrate binding.** In cytosol, inactive Akt exists as a folded molecule with the PH and regulatory domains covering parts of the kinase domain. Akt is recruited to the plasma membrane through the interaction of its PH domain with PIP_3. The membrane interaction results in a conformational change, moving the PH and regulatory domains away from the kinase domain and exposing Thr^{308} and Ser^{473} for phosphorylation by upstream kinases. When Akt is activated by phosphorylation at both sites, the PH domain closes, possibly enabling the separation of Akt from the membrane. The regulatory domain, which remained open, allows the substrate entry, and upon substrate binding the regulatory domain returns to a closed conformation as in the inactive form. *PIP2*, phosphatidylinositol 4,5-bisphosphate; *PI3K*, phosphatidylinositol 3-kinase; *pS*, phosphoserine; *pT*, phosphothreonine.

cross-linked pair $Lys2^{84}$-Lys^{426} within the distance constraint of 24 Å in both membrane-interacted and activated forms indicates that Lys^{284} and Lys^{426} moved farther away from each other during activation, at least by 16 Å, considering the reported distance between the corresponding residues (7.8 Å) from the crystal structure of inactive Akt2 (Table I). The crystal structure has revealed that the binding pockets for the substrate peptide and ATP, located within the activation loop and at the interface between the N-lobe (containing β1–5, αB, and αC) and C-lobe (mainly an α-helix), respectively, are blocked in the inactive Akt2 molecule (15, 16) with the C-terminal chain covering part of the ATP binding site. In addition, it has been suggested that residues such as Phe^{439} of the regulatory domain assist stabilization of the blocking conformation (15), and a dramatic conformational change to unblock these binding sites is required for Akt activation (15, 16). According to our data such dramatic displacement of the regulatory domain was introduced by the interaction with membrane, uncovering the binding pockets, and this open conformation was sustained after phosphorylation. Most probably, this open conformation allows substrate entry to the kinase domain, serving as an important determinant for the activated state of Akt in cytosol. The presence of cross-linked pair Lys^{284}-Lys^{426} after binding to GSK3β peptide and AMP-PNP suggests that a closed conformation was reestablished upon substrate binding. Although it is not easily explicable how peptide binding changes the conformation so dramatically, this result appeared to be in agreement with the crystal structure of Akt2, which was activated by Thr^{309} phosphorylation and S474D mutation and complexed with GSK3β peptide and AMP-PNP, where the distance between Lys^{285} and Lys^{427} was indicated to be 7.0 Å (Protein Data Bank entry 1o6k) (11).

In summary, our results strongly suggest that Akt undergoes distinctive conformational changes at each step of activation sequence. Based on our data, the following activation scheme is proposed (Fig. 7). Inactive Akt exists with a folded structure in cytoplasm with the PH and regulatory domains covering the kinase domain at least in part. Membrane translocation causes conformational changes of Akt so that both PH and regulatory domains become separated from the kinase domain to expose Thr^{308} and Ser^{473} for phosphorylation. Phosphorylation of Akt presumably triggers the separation of the PH domain from membrane, releasing Akt to the cytoplasm. The open conformation of the regulatory domain in the activated form of cytosolic Akt allows substrate entry, which is an important determinant for the activated state of Akt. This model is consistent with the well accepted notion that Akt activity correlates with conformational changes allowing phosphorylation at Thr^{308} and Ser^{473} (1, 5). Furthermore our model may offer an explanation for the previous findings that Ser^{474} phosphorylation is required for full activation of Akt2 (11) by depicting the regulatory domain moved away from the kinase domain after phosphorylation, allowing facilitated substrate entry and enhancing overall activity.

In conclusion, our results provide the first demonstration for the dramatic interdomain conformational changes in the full-length Akt structure in solution during activation and substrate binding. Our results also provide valuable complementary information to the crystal structures of this molecule. More importantly, our results set up a stage for the further investigation on

Akt-membrane, Akt-protein, and/or Akt-drug interactions that is the key to understand the molecular mechanisms involved in physiological and pathophysiological processes of cell survival.

* The costs of publication of this article were defrayed in part by the payment of page charges. This article must therefore be hereby marked "*advertisement*" in accordance with 18 U.S.C. Section 1734 solely to indicate this fact.

‡ To whom correspondence should be addressed: Section of Mass Spectrometry, Laboratory of Membrane Biophysics and Biochemistry, NIAAA, National Institutes of Health, 5625 Fishers Lane, Bethesda, MD 20892-9410. Tel.: 301-402-8746; Fax: 301-594-0035; E-mail: hykim@nih.gov.

REFERENCES

1. Brazil, D. P., and Hemmings, B. A. (2001) Ten years of protein kinase B signalling: a hard Akt to follow. *Trends Biochem. Sci.* **26,** 657–664
2. Lawlor, M. A., and Alessi, D. R. (2001) PKB/Akt: a key mediator of cell proliferation, survival and insulin responses? *J. Cell Sci.* **114,** 2903–2910
3. Staal, S. P. (1987) Molecular cloning of the Akt oncogene and its human homologues Akt1 and Akt2: amplification of Akt1 in a primary human gastric adenocarcinoma. *Proc. Natl. Acad. Sci. U. S. A.* **84,** 5034–5037
4. Bellacosa, A., Testa, J. R., Staal, S. P., and Tsichlis, P. N. (1991) A retroviral oncogene, Akt, encoding a serine-threonine kinase containing an SH2-like region. *Science* **254,** 274–277
5. Alessi, D. R., and Cohen, P. (1998) Mechanism of activation and function of protein kinase B. *Curr. Opin. Genet. Dev.* **8,** 55–62
6. Thomas, C., C., Deak, M., Alessi, D. R., and van Aalten, D. M. F. (2002) High-resolution structure of the pleckstrin homology domain of protein kinase B/Akt bound to phosphatidylinositol (3,4,5)-trisphosphate. *Curr. Biol.* **12,** 1256–1262
7. Stokoe, D., Stephens, L. R., Copeland, T., Gaffney, P. R. J., Reese, C. B., Painter, G. F., Holmes, A. B., McCormick, F., and Hawkins, P. T. (1997) Dual role of posphatidylinositol-3,4,5-trisphosphate in the activation of protein kinase B. *Science* **277,** 567–570
8. Andjelkovic, M., Alessi, D. R., Meier, R., Fermandez, A., Lamb, N. J. C., Frech, M., Cron, P., Cohen, P., Lucocq, J. M., and Hemmings, B. A. (1997) Role of translocation in the activation and function of protein kinase B. *J. Biol. Chem.* **272,** 31515–31524
9. Bellacosa, A., Chan, T. O., Ahmed, N. N., Datta, K,. Malstrom, S., Stpkoe, D., McCormick, F., Feng, J. N., and Tsichlis, P. (1998) Akt activation by growth factors is a multiple-step process: the role of the PH domain. *Oncogene* **17,** 313–325
10. Watton, S. J., and Downward, J. (1999) Akt/PKB localisation and 3′ phosphoinositide generation at sites of epithelial cell-matrix and cell-cell interaction. *Curr. Biol.* **9,** 433–436
11. Yang, J., Cron, P., Thompson, V., Good, V. M., Hess, D., Hemmings, B. A., and Barford, D. (2002) Molecular mechanism for the regulation of protein kinase B/Akt by hydrophobic motif phosphorylation. *Mol. Cell* **9,** 1227–1240
12. Datta, S. R., Brunet, A., and Greenberg, M. E. (1999) Cellular survival: a play in three Akts. *Genes Dev.* **13,** 2905–2927
13. Datta, S. R., Dudek, H., Tao, X. Masters, S. Fu, Haian, Gotoh, Y., and Greenberg, M. E. (1997) Akt phosphorylation of BAD couples survival signals to the cell-intrinsic death machinery. *Cell* **91,** 231–241
14. Milburn, C. C., Deak, M., Kelly, S. M., Price, S. M., Alessi, D. R., and van Aalten, D. M. F. (2003) Binding of phosphatidylinositol 3,4,5-trisphosphate to the pleckstrin homology domain of protein kinase B induces a conformational change. *Biochem. J.* **375,** 531–538
15. Huang, X., Begley, M., Morgenstern, K., A., Gu, Y., Rose, P., Zhao, H., and Zhu, X. (2003) Crystal structure of an inactive Akt2 kinase domain. *Structure* (*Lond*.) **11,** 21–30
16. Yang, J., Cron, P., Good, V. M., Thompson, V., Hemmings, B. A., and Barford, D. (2002) Crystal structure of an activated Akt/protein kinase B ternary complex with GSK3-peptide and AMP-PNP. *Nat. Struct. Biol.* **12,** 940–944
17. Auguin, D., Barthe, P., Auge-Senegas, M., Stern, M., Noguchi, M., and Roumestand, C. (2004) Solution structure and backbone dynamics of the pleckstrin homology domain of the human protein kinase B (PKB/Akt): interaction with inositol phosphates. *J. Biomol. NMR* **28,** 137–155
18. Calleja, V., Ameer-beg, S. M., Vojnovic, B., Woscholski, R., Downward, J., and Larijani, B. (2003) Monitoring conformational changes of proteins in cells by fluorescence lifetime imaging microscopy. *Biochem. J.* **372,** 33–40
19. Young, M. M., Tang, N., Hempel, J. C., Oshiro, C. M., Taylor, E. W., Kuntz, I. D., Gilson, B. W., and Dollinger, G. (2000) High throughput protein fold identification by using experimental constraints derived from intramolecular cross-links and mass spectrometry. *Proc. Natl. Acad. Sci. U. S. A.* **97,** 5802–5806
20. Taverner, T., Hall, N. E., Ohair, R. A. J., and Simpson, R. J. (2002) Characterization of an antagonist interleukin-6 dimer by stable isotope labeling, cross-linking, and mass spectrometry. *J. Biol. Chem.* **277,** 46487–46492
21. Back, J. W., de Jong, L., Muijsers, A. O., and Koster, C. G. (2003) Chemical cross-linking and mass spectrometry for protein structural modeling. *J. Mol. Biol.* **331,** 303–313
22. Huang, B. X., Dass, C., and Kim, H.-Y. (2005) Probing conformational changes of human serum albumin due to unsaturated fatty acid binding by chemical cross-linking and mass spectrometry. *Biochem. J.* **387,** 695–702
23. Silva, R. A. G., Hilliard, G. M., Fang, J., Macha, S., and Davidson, W. S. (2005) A three-dimensional molecular model of lipid-free apolipoprotein A-I determined by cross-linking/mass spectrometry and sequence threading. *Biochemistry* **44,** 2759–2769
24. Bennett, K. L., Kussmann, M., Bjork, P., Godzwon, M., Mikkelsen, M., Sorensen, P., and Roepstorff, P. (2000) Chemical cross-linking with thiol-cleavable reagents combined with differential mass spectrometric peptide mapping—a novel approach to assess intermolecular protein contacts. *Protein Sci.* **9,** 1503–1518
25. Sinz, A. (2003) Chemical cross-linking and mass spectrometry for mapping three-dimensional structures of proteins and protein complexes. *J. Mass Spectrom.* **38,** 1225–1237
26. Zhang, X., Wehbi, H., and Roberts, M. F. (2004) Cross-linking phosphatidylinositol-specific phospholipase C traps two activating phosphatidylcholine molecules on the enzyme. *J. Biol. Chem.* **279,** 20490–20500
27. Giron-Monzon, L., Manelyte, L., Ahrends, R., Kirsch, D., Spengler, B., and Friedhoff, P. (2004) Mapping protein-protein interactions between MutL and MutH by cross-linking. *J. Biol. Chem.* **279,** 49338–49345
28. Chu, F., Shan, S., Moustakas, D. T., Alber, F., Egea, P. F., Stroud, R. M., Walter, P., and Burlingame, A. L. (2004) Unraveling the interface of signal recognition particle and its receptor by using chemical cross-linking and tandem mass spectrometry. *Proc. Natl. Acad. Sci. U. S. A.* **101,** 16454–16459
29. Huang, B. X., Dass, C., and Kim, H.-Y. (2004) Probing three-dimensional structure of bovine serum albumin by chemical cross-linking and mass spectrometry. *J. Am. Soc. Mass Spectrom.* **15,** 1237–1247
30. Yao, X., Freas, A., Ramirez, J., Demirev, P. A., and Fenselau, C. (2001) Proteolytic ^{18}O labeling for comparative proteomics: model studies with two serotypes of adenovirus. *Anal. Chem.* **73,** 2836–2842
31. Back, J. W., Notenboom, V., Koning, L., J., Muijsers, A. O., Sixma, T. K., Koster, C. G., and Jong, L. (2002) Identification of cross-linked peptides for protein interaction studies using mass spectrometry and ^{18}O labeling. *Anal. Chem.* **74,** 4417–4422
32. Kim, H.-Y, Bigelow, J., and Kevala, J. H. (2004) Substrate preference in phosphatidylserine biosynthesis for docosahexaenoic acid containing species. *Biochemistry* **43,** 1030–1036
33. Alessi, D. R., James, S. R., Downes, C. P., Holmes, A. B., Gaffney, P. R. J., Reese, C. B., and Cohen, P. (1997) Characterization of a 3-phosphoinositide-dependent protein kinase which phosphorylates protein kinase Bα. *Curr. Biol.* **7,** 261–269
34. Schilling, B., Row, R. H., Gilbon, B. W., Guo, X., and Yong, M. M. (2003) MS2assign, automated assignment and nomenclature of tandem mass spectrometry of chemically cross-linked peptides. *J. Am. Soc. Mass Spectrom.* **14,** 834–850